Geo-Regioning for UWB Networks

Frank Althaus, Florian Troesch and Armin Wittneben
Communication Technology Laboratory, ETHZ, CH-8092 Zuerich
Telephone: +41 1 632 6918, Fax: +41 1 632 1209
Email: {althaus, troeschf, wittneben}@nari.ee.ethz.ch

***Abstract*— Ultra-Wideband provides high temporal resolution of multipath components of the propagation channel. Therefore a channel impulse response obtained from a certain transmitter can be seen as a signature of its position. This work investigates the possibility to perform rough localization in rich multipath environment by means of those signatures. We refer to geo-regioning as the intention to associate a received signature to a certain region in a room. A measurement campaign has been performed collecting a huge number signatures in 22 different regions in a warehouse-like scenario. By means of the measured data the performance of the geo-regioning approach is demonstrated. A simple geo-regioning algorithm is proposed and the impact of important algorithm parameters is pointed out.**

I. Introduction

One of the most cited advantages of Ultra-Wideband (UWB) technology is the accurate localization capability. The huge bandwidth introduces a very high temporal resolution of multipath components in the propagation channel including an accurate representation of the initial delay. Therefore, most localization and ranging approaches in UWB are based on time-of-arrival (ToA) estimation. In typical line-of-sight (LOS) conditions the first path (initial delay) is the strongest path and corresponds to the LOS component. However, if the first path does not correspond to the strongest path, more sophisticated algorithms are required to achieve an accurate estimate of the initial delay [1]. A general problem of the ToA approach is that the performance of the localization/ranging systems decreases very fast in non-LOS (NLOS) conditions since here the first arriving path may not correspond to the direct path and includes an additional detouring delay [2].
In this work we will follow a different approach exploiting the UWB nature of the channel to achieve a rough localization for some specific applications. We suppose that the channel impulse response (CIR) of a transmitter/receiver (TX/RX) pair is almost unique, given by many resolvable multipath components that result from the individual geographical constellation of RX and TX. At a certain RX the CIR received from any TX is like a signature of the TX position. If two TXs have a very similar signature they are very close together. Although it has been shown, that the spatial correlation of the signatures strongly decreases within about 10 cm [3], we will see that there remains enough information to decide whether two signatures belong to the same geographical region or not. We refer to this approach as "geo-regioning". We assume that a region can have a size of several dm^3 up to several m^3. Blind geo-regioning does not use a priori location information. It has many interesting applications such as (i) data fusion in dense sensor networks and (ii) routing in hierarchical sensor networks, where the clusterheads may base the routing selection on the region information. In data aided geo-regioning the position of some specific reference nodes in the network is known. This information is used to derive the position location information of all received signals by means of an appropriate regioning process. This facilitates a variety of location aware services and protocols in dense ad hoc networks.

In our geo-regioning approach we will only consider the shape of the signatures given by the relative positions of the multipath components but not the absolute temporal positions. Compared to the ToA based techniques, for the geo-regioning approach much more relaxed timing and synchronization accuracy is sufficient. Further, there is no special protocol required for the transmitters to be localized as it is, e.g., for ranging [1]. Since there are only estimates of the signatures required at the receiver, heterogeneous types of UWB transmitters as, e.g., sensors, tags or communication devices can be localized. Although the performance of such a system can be increased using several receivers at different positions (as it is usual in localization systems [4][5]), only one receiver is sufficient for the geo-regioning. Finally, geo-regioning is a promising approach for localization in environments where no direct path can be received.
The aim of this paper is to show the principle feasibility of the geo-regioning approach. We will show that the knowledge of the average power delay profiles of the different regions is sufficient to perform the regioning decision with reasonable reliability. This means that the average power delay profiles contain enough information to enable a proper differentiation between signatures originating from different regions and, at the same time, there are enough similarities between the signatures originating from a single region to detect this single region. It is obvious that the feasibility and performance of the geo-regioning approach depend very much on the characteristics of the propagation channel and environment, respectively. Therefore, a measurement campaign has been performed which provides an appropriate set of data to investigate the geo-regioning approach by means of real data [6].
The measurement campaign is briefly summarized in Section II. In Section III we introduce a first geo-regioning algorithm which uses full a priori knowledge of the average power delay profiles of the regions. We finally show initial performance

results in Section IV and conclude in Section V.

II. Measurements

A. Measurement setup and scenario

The measurements that are performed in this work are explicitly done to support investigations on the geo-regioning function. The intention of the measurements was to consider a number of selected regions in a room where a high number of CIRs are collected for each region. The exact position of the transmitter inside a region is not required.

A time-domain MIMO measurement setup using correlation method with 4 TX and 3 RX antennas is used. The spacing of the antennas was $d \geq 20$cm. TX and RX array were mounted in a height of 180cm. On the transmitter side 4 pseudo random bit sequence generators are running in parallel. The bit sequences are temporally shifted by at least 250ns to each other. This corresponds to a path length of 75m. We assume that the power of paths with higher length is negligible for our considerations. The TX antenna array was mounted on a two dimensional positioner which itself was placed on a wagon. The postioner allows to move the array in an area of 270mm x 560mm. The wagon was placed in a wide spacing at many positions in the room. We associate to each position of the wagon a certain region (see Fig. 2. The RX array was placed on a tripod at a fixed position in the room. Three parallel channels of a real time sampling scope (Lecroy SDA 6020) are used, sampling at a frequency of 20GHz. The trigger at the scope is not synchronized with the positioner of the TX array. That means that exact positions of the TX antennas are not known. However, since the array is moved by the positioner when the position of the wagon is fixed, the measured CIRs are located insight the region of the wagon. Since triggering at the scope is done periodically and the speed of the array is approximately constant the measured points have nearly equidistant spacing. The spacing is about 1.7cm and the speed of the positioner is of about 1cm/s. All measurements have been done in a cellar room of building ETF at ETH Zurich which could be seen as a warehouse-like scenario. The room has a size of about 7.4m x 45m and the height is about 6m. Only one half of the room was used for the measurements. There are many products of various stature and material stored in the room. The room is full of metallic objects as, e.g., large metallic shelves, heating pipes and metal cores but there were hardly any continuously wave blocking objects as, e.g., walls or cabinets, which may be a significant difference to the industrial environment presented in [7]. Fig. 1 shows a picture of the room. Fig. 2 shows a floor plan of the room including some details on the furniture with the positions of the wagon and the position of the receive array. Due to the chosen position of the RX array we have typical LOS regions from Region 01 to 11 and in Region 13 and 14. Typical NLOS region are from number 16 to 21.

A number of roughly 150 trigger events have been performed for each region. Since each trigger means $4 \cdot 3 = 12$ channel impulse responses this yields to a number of $12 \cdot 150 = 1800$ CIRs per region. The wagon was placed at 22

Fig. 1. Picture of the measurement room

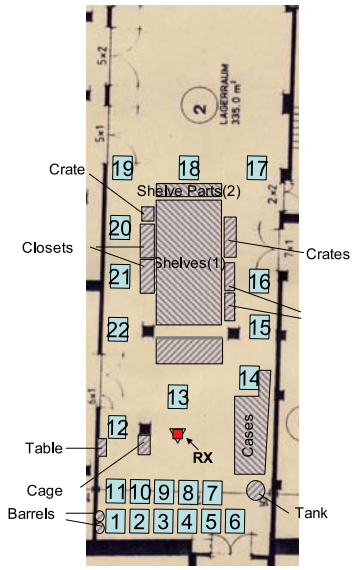

Fig. 2. Positions of RX array and wagon

different positions. So, a total number of 39600 CIRs have been collected. This set of data provides the basis for our geo-regioning investigations. As a first step, in this paper only single antenna links are considered. Future investigations will take the impact of multiple antenna systems into account.

B. Power delay profile and average power delay profile

In Section III a geo-regioning algorithm will be proposed which is based on the average power delay profiles (APDP) of the regions. The APDP of a Region A is determined by

$$\text{APDP}_A(k) = \frac{1}{N_A} \sum_{m=1}^{N_A} |h_{A,m}(k)|^2, \qquad (1)$$

where N_A is the number of available measurements of impulse responses or signatures from Region A represented by the sampled series $h_{A,m}(k)$. The m-th PDP of Region A is then $|h_{A,m}(k)|^2, k = 1...K$. In Fig. 3 a section of the PDPs of the LOS Regions 03 and the NLOS Region 18 is depicted. The contour plot shows high values with dark colors and

low values with light colors. The index is the number (m) of the measurement in the region. Since the absolute temporal position of the CIRs have not been measured the PDPs are aligned by their maximum values. The clear LOS nature of Region 03 can be observed since the first peak at time 15ns is very strong and is clearly the maximum. After that peak, several clusters are visible which may be significant for that region. In the lower part, for the NLOS Region 18 the alignment is much more difficult. Some mistakes in the alignment can be observed, e.g. at indices 37 and 122. At higher indices (> 100) two dominant peaks appear. Many clusters can be observed before the maximum peak arrives and several can be seen after it. In Fig. 4 the APDPs are shown. The received power of Region 03 is much higher than that of Region 18 which is located farther away from the RX position (see Fig. 2). Beside the difference in the received power, the shape of these sections of the APDPs look very different. In Fig. 5 the APDPs of two NLOS regions, Region

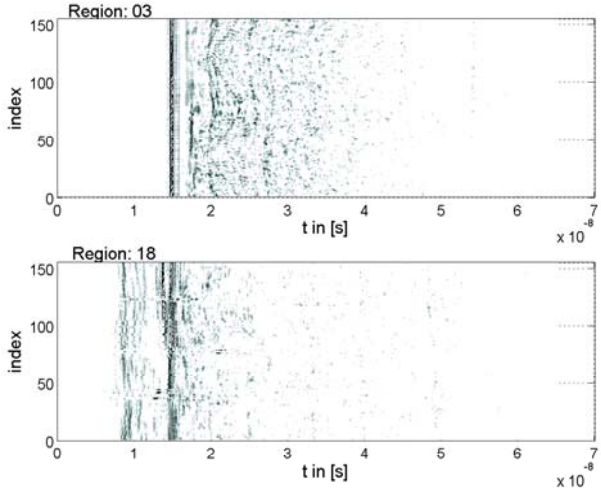

Fig. 3. PDPs of Regions 03 and 18

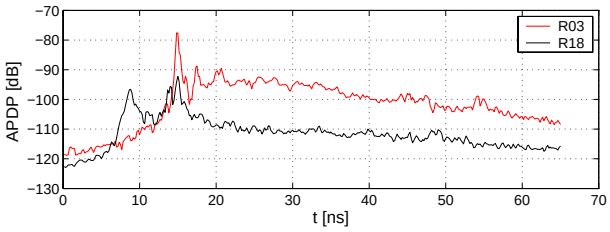

Fig. 4. APDPs of Regions 03 and 18

17 and 19, are shown. Both regions have almost the same distance to the receiver and are located almost symmetrically in the room (see Fig. 2). Although the APDPs look quite similar, significant differences which are indicated by the arrows can be observed. These considerations motivate the algorithm proposed in Section III.

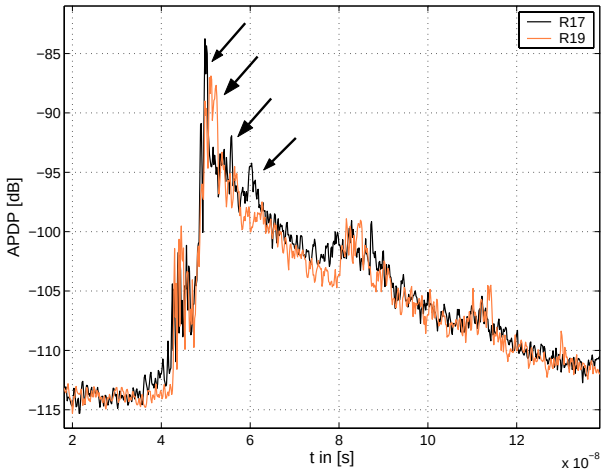

Fig. 5. APDPs of Regions 17 and 19

III. A SIMPLE GEO-REGIONING ALGORITHM

In this paper we consider the geo-regioning application where a rough localization of the transmitter is requested as described in Section I. That means that a transmitter has to be localized by associating its position to a region just by means of its signature. The main goal here is to propose a simple algorithm proving the principle feasibility of such a geo-regioning approach.

We assume that the average power delay profiles (APDP) of all regions are a priori known at the receiver. To derive a simple algorithm detecting the region by the signature we make the following simplifying assumption:

Each signature $x(k)$ with $k = 1...K$ is an outcome from a random process that generates statistically independent Gaussian variables. The Gaussian distribution is zero mean and the variance at index k is depending on the region where the signature originates and is set to the corresponding APDP value:

$$\sigma^2(k) := \text{APDP}(k) \tag{2}$$

So, the probability density for $x(k)$ which is originated from Region A is $\mathcal{N}(0, \sigma_A^2(k))$:

$$p(x(k)|A) = \frac{1}{\sqrt{2\pi}\sigma_A(k)} \cdot \exp\left(-\frac{x^2(k)}{2\sigma_A^2}\right) \tag{3}$$

A maximum likelihood (ML) estimator that considers all possible regions $\mathcal{A}$ maximizes the probability density

$$\max_{\mathcal{A}} p(\vec{x}|\mathcal{A}), \tag{4}$$

with $\vec{x}[k] = x(k), k = 1...K$. The ML estimator deciding between two regions A and B is:

$$p(\vec{x}|A) \underset{B}{\overset{A}{\gtrless}} p(\vec{x}|B), \tag{5}$$

Since the samples $x(k)$ are assumed to be statistically independent the log-likelihood can be derived:

$$\prod_{k=1}^{K} p(x(k)|A) \underset{B}{\overset{A}{\gtrless}} \prod_{k=1}^{K} p(x(k)|B) \tag{6}$$

$$\Leftrightarrow \sum_{k=1}^{K} \ln\left(\frac{1}{\sqrt{2\pi}\sigma_A(k)} \cdot \exp\left(-\frac{x^2(k)}{2\sigma_A^2}\right)\right) \underset{B}{\overset{A}{\gtrless}} \sum_{k=1}^{K} \ln\left(\frac{1}{\sqrt{2\pi}\sigma_B(k)} \cdot \exp\left(-\frac{x^2(k)}{2\sigma_B^2}\right)\right)$$

$$\Leftrightarrow \sum_{k=1}^{K} x^2(k) \frac{\sigma_A^2(k) - \sigma_B^2(k)}{\sigma_A^2(k)\sigma_B^2(k)} \underset{B}{\overset{A}{\gtrless}} \sum_{k=1}^{K} \ln \frac{\sigma_A^2(k)}{\sigma_B^2(k)} \tag{7}$$

IV. Performance results

In this section the performance of the algorithm is shown by means of simulations running with the measured data. As a performance measure we use the pairwise error probability when deciding between two regions. We assume that we have received a noisy estimate $v(k), k = 1...K$ of the signature $x(k)$, where the noise component $n(k)$ is assumed additive zero mean Gaussian with variance σ_n^2.

$$v(k) = x(k) + n(k) \tag{8}$$

$v(k)$ is the sum of two Gaussian distributed random variables. If we assume $x(k)$ originating from Region A, the probability density function is $\mathcal{N}(0, \sigma_A^2(k) + \sigma_n^2)$. With $\sigma_{A'}^2(k) = \sigma_A^2(k) + \sigma_n^2$ the ML estimator from (6) can be written as:

$$\sum_{k=1}^{K} x^2(k) \frac{\sigma_{A'}^2(k) - \sigma_{B'}^2(k)}{\sigma_{A'}^2(k)\sigma_{B'}^2(k)} \underset{B}{\overset{A}{\gtrless}} \sum_{k=1}^{K} \ln \frac{\sigma_{A'}^2(k)}{\sigma_{B'}^2(k)} \tag{9}$$

In Fig. 6 the pairwise error probability, $P_2(e)$, of Region 03 with some exemplary regions is plotted over the received SNR. 150 signatures originating from Region 03 and 150 originating from another region are taken from the measurements and added with white Gaussian noise. The detector of (9) is applied and its error performance is evaluated. The SNR is defined by the mean received power per signature over the noise power:

$$\text{SNR} = \frac{1}{\sigma_n^2} \cdot \frac{1}{N_A + N_B} \sum_{m=1}^{N_A+N_B} \sum_{k=1}^{K} |h_m(k)|^2 \tag{10}$$

Note that for CIR estimation we can expect 10dB to 15dB more SNR than for data detection. Region 03 is a LOS region whereas Regions 12 and 17 are NLOS regions. Their signatures show very few similarity to the signatures from Region 03 and achieve best performance. Regions 01 and 14 are LOS regions where the signatures have more similarities with the ones from Region 03. Compared to these regions the LOS Region 02 shows a poorer performance. This could be expected since it is very close to Region 03 and some of the measured positions where located only a few cm apart from

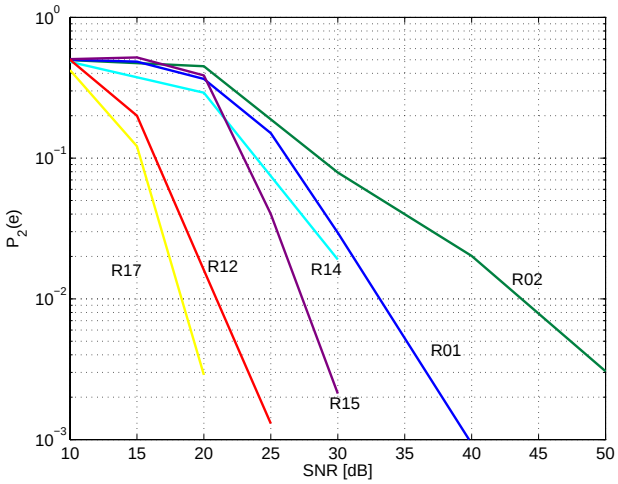

Fig. 6. Pairwise error probabilities for Region 03

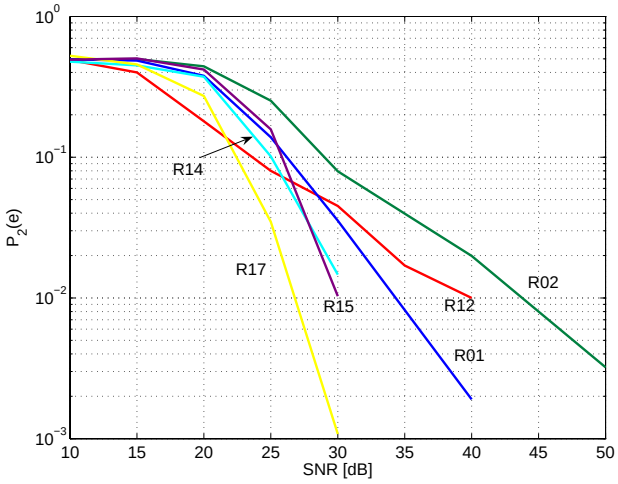

Fig. 7. Pairwise error probabilities for Region 03 with normalized receive energy

some positions of Region 03. Nevertheless, we conclude that many regions can be separated at reasonable receive SNR.

It is obvious that one main parameter to distinguish the regions is the received energy and in similar propagation conditions the distance of the regions to the receiver. In order to compare regions with similar received energy we have normalized the received energy per region since only a few of the measured regions show similar energy. Fig. 7 shows the same simulations as Fig. 6 but with normalized received energy. As expected the performance decreases for the regions that are located far away from Region 03 and have different path loss. However, for high SNR all regions, except of the direct neighbor Region 02 and Region 12, achieve $P_2(e) \leq 10^{-2}$ for SNR < 35dB. That means on the one hand that the signatures within one region have enough similarities to recognize them as belonging together. On the other hand the signatures in different regions differ as much as to recognize them belonging to different regions.

A. Impact of the bandwidth

Fig. 8 shows the impact of the bandwidth in use. As expected the performance increases with the bandwidth. For the measured scenario a bandwidth of $B > 200$MHz is required to achieve $P_2(e) < 10^{-2}$. This strengthens the assumption that this kind of localization is only possible in UWB systems (bandwidths $B \geq$500MHz).

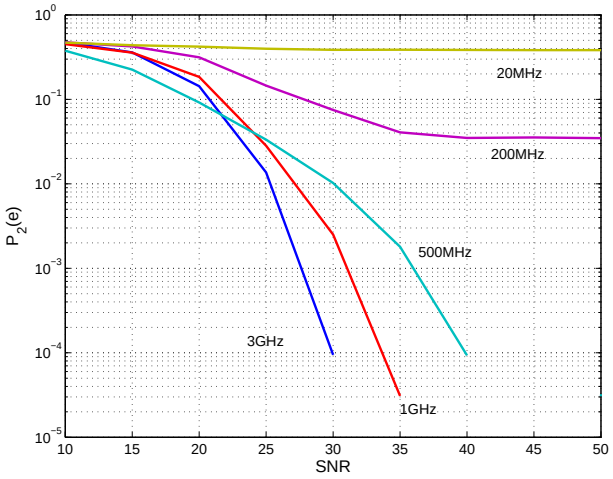

Fig. 8. Pairwise error probabilities for Region 15 and 17 for different bandwidth and normalized received energy

B. Impact of the length of the signatures

We investigate how the performance depends on the observation length of the signatures. Therefore, the signatures are aligned by a threshold value which is chosen such that the direct path lies above that threshold. A time window of a given length beginning at the point where the threshold is reached for the first time is used to cut a section of the signature. Fig. 9 shows the impact of the length of the signatures for several region pairs and various SNR. The length of the window ΔT_w grows from 5ns to 100ns. The performance tends to increase with increasing window length up to a length of $\Delta T_w = 40$ns. For Regions 13 and 15 an further improvement with increasing length can be observed. In case of the NLOS Regions 17 and 18 a significant difference in the APDPs appears within the first 10ns. The delay between the direct path and the maximum path is 1ns and 5ns, respectively. Therefore, the performance is quite good with small window length and remains almost unaffected with increasing length.

The plots in Figures 6 to 9 have shown exemplary error probabilities. However, similar results are achieved for all other LOS and NLOS regions. Note, that the presented algorithm and the simulated error performance are not optimum but show the principle feasibility of geo-regioning.

V. Conclusions

The concept of geo-regioning has been introduced. Measurements have been performed to support investigations

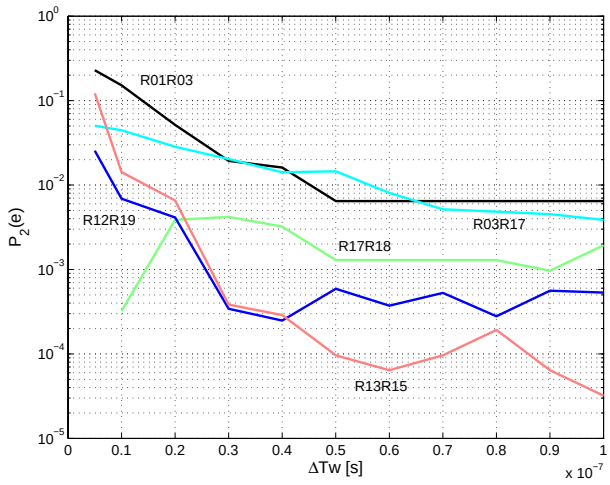

Fig. 9. Pairwise error probabilities in dependence of the length of the signatures for various SNR values

on geo-regioning. A simple geo-regioning algorithm with good performance has been introduced proving the principle feasibility of geo-regioning in a warehouse-like scenario. It has been shown that the required bandwidth is $B > 200$MHz which makes it applicable in particular in UWB systems. We conclude that the proposed geo-regioning approach achieves good performance for the measured scenario at reasonable receive SNR. The simplicity and the good performance of the approach make geo-regioning an attractive candidate for location aided services in UWB sensor and ad hoc networks. Future work will concern the improvement and complexity reduction of the geo-regioning algorithm, the estimation of the APDPs and the impact of using multiple antennas at TX and RX, respectively.

VI. Acknowledgement

This work has been supported by the European Integrated Project PULSERS. The authors would like to thank the partners.

References

[1] Joon-Yong Lee and Robert A. Scholtz. Ranging in a dense multipath environment using an UWB radio link. In *IEEE Journal on Selected Areas in Communications, Vol. 20, No.9*, pages 1677–1683, December 2002.

[2] B. Denis, J. Keignart, and N. Daniele. Impact of NLOS propagation upon ranging precision in UWB systems. In *IEEE Conference on Ultra Wideband Systems and Technologies*, pages 379 – 383, November 2003.

[3] C. Prettie, D. Cheung, and L. Ruschand M. Ho. Spatial correlation of UWB signals in a home environment. In *IEEE Ultra Wideband Systems and Technologies*, pages 65 – 69, May 2002.

[4] S. J. Ingram, D. Harmer, and M. Quinlan. Ultra wideband indoor positioning systems and their use in emergencies. In *Position Location and Navigation Symposium*, pages 706 – 715, April 2004.

[5] D. Niculescu. Positioning in ad hoc sensor networks. In *Network, IEEE*, pages 24 – 29, July/August 2004.

[6] F. Althaus, F. Troesch, and A. Wittneben. UWB geo regioning in rich multipath environment. In *IEEE Vehicular Technology Conference, VTC Fall 2005*, September 2005.

[7] J. Karedal, S. Wyne, P. Almers, F. Tufvesson, and A. Molisch. UWB channel measurements in an industrial environment. In *IEEE Globecom*, 2004.